Published in final edited form as:
Int J Cancer. 2010 May 15; 126(10): 2319–2329. doi:10.1002/ijc.24920.

Role of CXC Chemokine Ligand 13 in Oral Squamous Cell Carcinoma Associated Osteolysis in Athymic Mice

Subramanya N.M. Pandruvada[1], **Yuvaraj Sambandam**[1], **Xiang Liu**[2], **Kumaran Sundaram**[1], **Srinivasan Shanmugarajan**[1], **William L. Ries**[3], **James S. Norris**[2], **Steven D. London**[3], and **Sakamuri V. Reddy**[1]

[1] Charles P. Darby Children's Research Institute, Medical University of South Carolina, Charleston SC, USA

[2] Department of Microbiology and Immunology, Medical University of South Carolina, Charleston SC, USA

[3] College of Dental Medicine, Medical University of South Carolina, Charleston SC, USA

Abstract

Oral squamous cell carcinomas (OSCC) are malignant tumors with a potent activity of local bone invasion; however the molecular mechanisms of tumor osteolysis are unclear. In this study, we identified high level expression of chemokine ligand, CXCL13 and RANK ligand (RANKL) in OSCC cells (SCC1, SCC12 and SCC14a). OSCC cell conditioned media (20%) induced osteoclast differentiation which was inhibited by OPG in peripheral blood monocyte cultures indicating that OSCC cells produce soluble RANKL. Recombinant hCXCL13 (10 ng/ml) significantly enhanced RANKL stimulated osteoclast differentiation in these cultures. Trans-well migration assay identified that CXCL13 induces chemotaxis of peripheral blood monocytes *in vitro* which was inhibited by addition of anti-CXCR5 receptor antibody. Zymogram analysis of conditioned media from OSCC cells revealed matrix metalloproteinase-9 (MMP-9) activity. Interestingly, CXCL13 treatment to OSCC cells induced CXCR5 and MMP-9 expression suggesting an autocrine regulatory function in OSCC cells. To examine the OSCC tumor cell bone invasion/osteolysis, we established an *in vivo* model for OSCC by subcutaneous injection of OSCC cells onto the surface of calvaria in NCr-nu/nu athymic mice, which developed tumors in 4–5 weeks. μCT analysis revealed numerous osteolytic lesions in calvaria from OSCC tumor-bearing mice. Histochemical staining of calvarial sections from these mice revealed a significant increase in the numbers of TRAP-positive osteoclasts at the tumor-bone interface. Immunohistochemical analysis confirmed CXCL13 and MMP-9 expression in tumor cells. Thus, our data implicate a functional role for CXCL13 in bone invasion and may be a potential therapeutic target to prevent osteolysis associated with OSCC tumors *in vivo*.

Keywords

Oral squamous cell carcinoma (OSCC); Chemokine; MMP-9; Bone invasion; RANK ligand; Osteoclast; Mouse model

[*]Address for Correspondence: Sakamuri V. Reddy, Ph.D, Charles P. Darby Children's Research Institute, 173 Ashley Avenue, Charleston, SC 29425; Tel: Ph. 843-792-8373; Fax: 843-792-7466; reddysv@musc.edu.

Introduction

Head and neck squamous cell carcinoma (HNSCC) are the most common malignant neoplasms, with a prevalence estimated to be greater than 40,000 cases annually in the US. Oral squamous cell carcinoma (OSCC), which contributes to 40% of all HNSCC is associated with mucosal surfaces of the oral cavity and oropharynx 1. The etiology of OSCC involves both a genetic predisposition and exposure to environmental carcinogens such as tobacco, alcohol, chronic inflammation and viral infection 2. Curcumin has been shown to suppress HNSCC growth both in vitro and in vivo 3, and Fas-mediated apoptosis in HNSCC is a proven and efficient therapeutic approach in a xenograft animal model 4. Furthermore, tamoxifen inhibition of OSCC cell growth *in vitro* 5 and a role for human longevity assurance gene 1 (LASS1) and C_{18}-ceramide in chemotherapy induced cell death in HNSCC have been reported 6. Malignant HNSCC tumors are known to have a potent activity of local bone invasion; however the molecular mechanisms of tumor-associated osteolysis are unclear.

The osteoclast is hematopoietic in origin and is the bone-resorbing cell derived from monocyte/macrophage lineage. Tumor necrosis factor (TNF) family member, RANK ligand (RANKL), which is expressed on marrow stromal/osteoblast cells in response to several osteotropic factors, is critical for osteoclast precursor differentiation to form multinucleated osteoclasts, which resorb bone 7. Osteoclast activity is controlled by local factors produced in the bone microenvironment. In addition, the osteoclast is an autocrine/paracrine, intracrine regulatory cell that produces factors such as IL-6, annexin II, TGF-beta and OIP-1/hSca, which influence its own formation and activity. Matrix metalloproteinase-9 (MMP-9), a type IV collagenase is highly expressed in osteoclast cells and plays an important role in degradation of the extracellular matrix 8. Osteoclast activation plays an important role in several malignancies including oral cancers invasion of bone and subsequent metastasis 9. Further, studies using a murine mandibular bone invasion model for OSCC demonstrated mRNA expression of cytokines associated with osteoclast activation such as IL-6, TNF-α and PTHrP in tumor tissue as well as high bone resorption 9. Also, conditioned media from OSCC cells derived from patients with bone involvement stimulated osteoclast differentiation in vitro 10.

Chemokines are a superfamily of small, cytokine-like proteins that selectively attract and activate different cell types 11. CXC chemokines are known to promote angiogenesis 12 and have a characteristic heparin-binding domain. Chemokines interact with seven-transmembrane-domain glycoprotein receptors coupled to the G protein signaling pathway 11. In several studies, tumor cells were shown to express functionally active chemokine receptors which regulate cellular functions and metastasis 13. HNSCC has been reported to predominantly expressed chemokine receptors such as CCR7 and CXCR5; however, CXCR4 expression is low or undetectable 14. CXCL13 (BCA-1) which binds monogamously to the CXCR5 receptor and is involved in B-cell chemotaxis and is induced under inflammatory conditions 15. Microarray analysis for gene expression profiling in OSCC identified gene signatures which include chemokine (CXC motif) ligand-13 and matrix-metalloproteinases (MMPs) that are highly relevant to OSCC development and progression 16. However, a functional role for CXCL13 in HNSCC tumor cell invasion and osteolysis is unknown. In this study, we showed CXCL13 expression and an autocrine regulation of MMP-9 production in tumor cells. We further show CXCL13 and RANKL expression in OSCC cells support osteoclastogenesis. We developed an *in vivo* model for OSCC by subcutaneous injection of SCC 14a cells onto the surface of calvaria in NCr-nu/nu athymic mice which showed osteolytic lesions. Our data implicate CXCL13 a potential therapeutic target to prevent OSCC tumor-associated osteolysis *in vivo*.

Materials and Methods

Cell lines and culture

Human OSCC-derived cell lines SCC1, SCC12 and SCC14a were generously provided by Dr. Thomas E. Carey (University of Michigan, Ann Arbor, MI). The OSCC, normal human fibroblast cell lines, WI-38 and IMR-90 (ATCC, Manassas, VA) were maintained in Dulbecco's Modified Eagle Medium containing 10% fetal bovine serum (FBS) and supplemented with L-glutamine, penicillin, and streptomycin. The RWPE-1 (normal human prostatic epithelial cells) (ATCC, Manassas, VA) cells were grown in keratinocyte serum free medium (K-SFM) containing 50 μg/ml bovine pituitary extract and 5 ng/ml epidermal growth factor. All cells were incubated at 37 °C in 5% CO_2.

Quantitative real-time RT-PCR

CXCL13, CXCR5, RANKL and MMP-9 mRNA expression levels were determined by quantitative real-time reverse transcription polymerase chain reaction (RT-PCR) as described previously 17. Briefly, total RNA was isolated from OSCC cells using RNAzol reagent (Tel-Test Inc, Friendswood, TX). A reverse transcription reaction was performed using poly-dT primer and Moloney murine leukemia virus reverse transcriptase (Applied Biosystems) in a 25 μl reaction volume containing total RNA (2 μg), 1x PCR buffer and 2 mM $MgCl_2$, at 42 °C for 15 min followed by 95 °C for 5 min. The real-time PCR was performed using SYBR Green Supermix in an iCycler (iCycler iQ Single-color Real Time-PCR detection system; Bio-Rad, Hercules, CA). The primer sequences used to amplify GAPDH mRNA were 5′-TGC ACC ACC AAC TGC TTA GC-3′ (sense) and 5′-GGC ATG GAC TGT GGT CAT GAG-3′ (anti-sense); CXCL13 mRNA 5′-CAG TCC AAG GTG TTC TGG-3′ (sense) and 5′-CAA TGA AGC GTC TAG GGA TAA AG-3′ (anti-sense); CXCR5 mRNA 5′-CTT CGC CAA AGT CAG CCA AG -3′ (sense) and 5′-TGG TAG AGG AAT CGG GAG GT-3′ (anti-sense); RANKL mRNA 5′-ACC AGC ATC AAA ATC CCA AG -3′ (sense) and 5′-TAA GGA GGG GTT GGA GAC CT-3′ (anti-sense); MMP-9 mRNA 5′-TGA CAG CGA CAA GAA GTG-3′ (sense) and 5′-CAG TGA AGC GGT ACA TAG G-3′ (anti-sense). Thermal cycling at 94 °C for 3 min, followed by 40 cycles of amplifications at 94 °C for 30 s, 60 °C for 1 min, 72 °C for 1 min and 72 °C for 5 min as the final elongation step. Relative mRNA expression was normalized in all the samples analyzed with respect to the levels of GAPDH mRNA amplification.

Osteoclast differentiation assay

Human peripheral blood mononuclear cells (PBMC) were isolated from heparinized blood using Histopaque 1077 (Sigma, St Louis, MO) and resuspended in α-MEM with 10% FBS as described 18. Briefly, 15 ml of whole blood was mixed with 15 ml of warm (37 °C) α-MEM, layered over 15 ml of histopaque and centrifuged (1,500 × g, 30 min) at room temperature. The cell layer on top of the histopaque was collected, resuspended in 10 ml of α-MEM and centrifuged. The mononuclear cells collected were plated in 96-well plates at 6×10^5 cells per well in 0.2 ml of medium (α-MEM, pH 7.4, containing 10% FBS) supplemented with 10 ng/ml hM-CSF and presence of 100 ng/ml hRANKL or OSCC cell conditioned media (CM). The cells were re-fed twice weekly by semi-depletion (half of the medium withdrawn and replaced with fresh medium). At the end of culture period (10 days) the cells were fixed with 2% glutaraldehyde in PBS and stained for tartrate-resistant acid phosphatase (TRAP) activity using a histochemical staining kit (Sigma, St. Louis, MO) as described 19. TRAP-positive multinucleated cells containing three or more nuclei were scored as osteoclast cells under a microscope.

Chemotaxis assay

Chemotaxis of freshly isolated PBMC as described above was assessed in a 24-well plate containing polycarbonate membrane inserts with an 8-μm pore size (Costar Corning, NY) as described 20. Briefly, cell suspensions (4.5×10^3) of monocytes in culture medium were added to the upper chemotaxis chambers overlying wells containing medium with or without recombinant human CXCL13 (0–10 ng/ml). After 1 h incubation at 37 °C in 5% CO_2, cells that migrated into the lower chamber were counted using a hemocytometer.

Western blot analysis

OSCC cells were seeded in 6-well plates at a density of 5×10^5 cells per ml of DMEM containing 10% FBS and cultured for 48 h in the presence or absence of CXCL13 (10 ng/ml). The cells were lysed in RIPA buffer containing 1x protease inhibitor cocktail (Sigma, St. Louis, MO). Protein content of the samples was measured using the BCA reagent (Pierce, Madison, WI). Protein (20 μg) samples were then subjected to SDS-PAGE using 12% Tris HCl gels and blot transferred on to a nitrocellulose membrane. Blocking was performed with 5% non-fat dry milk in TBST buffer (50 mM Tris, pH 7.2, 150 mM NaCl; 0.1%Tween 20) for 1 h. The membrane was incubated with a primary anti-MMP-9 and anti-CXCR5 antibody at 1: 1000 dilution overnight at 4 °C. The blots were then incubated for 1 h with horseradish peroxidase conjugated secondary antibody and developed using an ECL system (Pierce, Madison, WI). β-actin expression levels in all the samples were used to normalize loading variations. The band intensity was quantified by densitometric analysis using the NIH ImageJ Program.

Gelatin zymography for MMP-9 activity

The conditioned media obtained from OSCC cells stimulated with and without CXCL13 (10 ng/ml) for 48 h were analyzed for MMP-9 activity by gelatin substrate gel electrophoresis as described earlier 21. Serum free cell cultured media samples were applied without reduction to a 10% polyacrylamide gel containing 0.1% gelatin. After electrophoresis, the gels were washed in washing buffer (50 mM Tris-HCl, pH 7.5; 5 mM $CaCl_2$, 1μM $ZnCl_2$ and 2.5% Triton X-100) for 30 min at room temperature, and then incubated overnight at 37 °C in the above buffer without Triton X-100. The gels were stained with a solution containing 0.1% Coomassie Brilliant Blue R-250. Formation of clear zone against the blue background on the polyacrylamide gels indicated the gelatinolytic activity, which was quantified by densitometric analysis using the NIH ImageJ Program.

CXCL13 shRNA knock-down

CXCL13 expression in SCC14a cells was knock-down using SureSilencing shRNA plasmid obtained from SABiosciecnes Frederick, MD. CXCL13 targeting sequence in the plasmid was 5′-ATCCCTAGACGCTTCATTGAT-3′ and the scrambled sequence in the control shRNA plasmid was 5′-GGAATCTCATTCGATGCATAC-3′. SCC14a cells were stably transfected with shRNA containing vectors by lipofectamine and clonal cell lines were established by selection with neomycin (800 μg/ml). shRNA suppression of CXCL13 production and mRNA expression were confirmed by ELISA and real-time RT-PCR as described.

In vivo model for OSCC

Athymic NCr-nu/nu male mice, aged 4 to 6 weeks (NCI, Frederick, MD) were used to develop an *in vivo* model for OSCC tumor cell invasion into bone and osteolysis. Under sterile conditions, 7×10^6 OSCC cells in phosphate buffered saline (PBS) were injected subcutaneously (n=10) overlaying the calvaria and PBS alone injected were as served control group (n=8). Tumor development over calvaria was monitored weekly using vernier

calipers. Animals were sacrificed when the tumor reached 2000 mm^3. At the end of experimental period, the animals were sacrificed and calvaria were collected for μCT analysis. Tumor were surgically removed and fixed in formalin for histological analysis.

Micro-computed tomography (μCT) imaging

Calvaria were surgically removed from PBS treated control, SCC14a, SCC12 tumors-bearing athymic mice were fixed in 70% ethanol and scanned using a Skyscan 1072 μCT instrument (Skyscan, Antwerp, Belgium). μCT-Analyser software (from SkyScan) was used to analyze the structure of the sample using the global segmentation method. Two-dimensional images were used to generate three-dimensional reconstructions with the software supplied with the instrument.

Histologic analysis

Formalin-fixed SCC14a tumor specimens collected from athymic mice were processed for paraffin sectioning. Serial 5-μm sections were cut on a modified Leica RM 2155 rotary microtome (Leica Microsystems, Ontario, Canada) and stained with hematoxylin and eosin. Immunocytochemical staining of the sections were performed by incubation of serial sections with anti-CXCR5, anti-CXCL13 or anti-MMP-9 antibody in 5% BSA overnight followed by HRP labeled secondary antibody and DAB staining. Specimens treated with non-specific IgG served as control.

To perform histochemical staining, tumor-bearing calvaria were decalcified in 0.5 M EDTA (pH 7.4) for a 1–3 week period and processed for paraffin embedding. Serial 4 to 6-μm sections of paraffin embedded calvaria were stained for TRAP activity. Histomorphometric analysis of TRAP-positive osteoclast numbers at the tumor-bone interface was performed with OsteoMeasure version 2.2 software.

Quantification of CXCL13

CXCL13 levels in OSCC, RWPE-1, WI-38 and IMR-90 cells-conditioned media (CM) were measured using an ELISA kit (R&D systems, Minneapolis, MO) following the manufacturer's protocol.

Statistical analysis

Results are represented as mean±SE of at least three independent experiments. Differences between experimental groups were analyzed by ANOVA using Graphpad Prism software. Values were considered significantly different for $*p<0.05$.

Results

CXCL13 and CXCR5 expression in OSCC cells

Chemokines are implicated in tumor progression and metastasis 22. Recent evidence indicated down regulation of CXCL5 expression inhibits HNSCC development and bone invasion 23. In this study, we examined CXCL13 and CXCR5 expression in OSCC derived cell lines (SCC1, SCC12 and SCC14a). ELISA analysis of conditioned media (CM) obtained from OSCC cell lines revealed CXCL13 at significantly high (38 to 118 pg/ml) concentration. In contrast, normal epithelial and fibroblast cells produced low levels (18 to 25 pg/ml) of CXCL13 (Fig. 1A). We further examined CXCL13 and CXCR5 receptor mRNA expression in OSCC cells by real-time RT-PCR analysis. CXCL13 mRNA expression was abundant in SCC1 and SCC14a; but at very low levels in SCC12 cells. CXCR5 mRNA is expressed at high levels in all the OSCC cell lines analyzed (Fig. 1B). We further examined whether CXCL13 stimulates CXCR5 mRNA expression in OSCC cells.

OSCC cells were stimulated with different concentration of CXCL13 (0–25 ng/ml) for 48 h. Real-time PCR analysis of total RNA isolated from these cells identified a dose-dependent stimulation of CXCR5 mRNA expression (Fig. 1C). Western blot analysis of total cell lysates further confirmed CXCL13 stimulation of CXCR5 expression in OSCC cells (Fig. 1D). Thus, our results implicate CXCL13/CXCR5 expression in OSCC and suggest an autocrine regulatory role for CXCL13 for enhancing CXCR5 receptor expression in OSCC cells.

OSCC cells support osteoclast formation

Tumor cells activate bone resorbing osteoclasts, thereby facilitating osteolytic process and bone invasion24. RANKL is a critical osteoclastogenic factor in the bone microenvironment 7. To determine the potential of OSCC cells to stimulate osteoclast formation, CM collected from these cells was tested at 1 and 20% concentrations for its capacity to stimulate osteoclast formation in peripheral blood mononuclear cell (PBMC) cultures as described in the methods. Treatment of PBMC with SCC14a cell CM at a 20% concentration in the presence of M-CSF (10 ng/ml) significantly increased (190±23) TRAP positive multinucleated cell formation compared to control cultures treated with M-CSF alone (8±2) in the absence of RANKL. Osteoclasts formed in PBMC cultures stimulated with RANKL (100 ng/ml) and M-CSF (10 ng/ml) served as a positive control (321±32) (Fig. 2A). Osteoprotegerin (OPG) is a decoy receptor of RANKL which inhibits RANKL stimulated osteoclast differentiation25 and addition of OPG significantly inhibited osteoclast formation compared to OSCC-CM alone in these cultures (Fig. 2B). These data suggest that the OSCC cells produce significant levels of RANKL, thereby stimulating osteoclast differentiation. Real-time RT-PCR analysis further confirmed RANKL mRNA expression in OSCC cells (Fig. 2C).

CXCL13 stimulates MMP-9 expression in OSCC cells

Tumor cell production of MMP-9 facilitates bone invasion 26. Therefore, we further examined MMP-9 expression and the potential of CXCL13 to up regulate MMP-9 expression in OSCC cells. Zymogram analysis of CM obtained from OSCC cell lines (SCC14a, SCC1 and SCC12) stimulated with CXCL13 for 48 h demonstrated a significant increase in the levels of MMP-9 activity (Fig. 3A). Total RNA isolated from OSCC cells treated with recombinant CXCL13 (0–25 ng/ml) for a 48 h period were subjected to real-time PCR analysis for MMP-9 mRNA expression. As shown in Fig. 3B, OSCC cells stimulated with CXCL13 demonstrated a dose-dependent increase in the levels of MMP-9 mRNA expression. Western blot analysis of total cell lysates obtained from these cells further confirmed CXCL13 stimulation of MMP-9 expression in a dose-dependent manner (Fig. 3C). Further, OSCC cells stimulated with CXCL13 in the presence of anti-CXCR5 antibody showed a significant decrease in the levels of MMP-9 expression (Fig. 3D). These data indicate that the CXCL13/CXCR5 axis play an important role in bone invasion through upregulation of MMP-9 expression in OSCC cells.

CXCL13 promotes chemotactic recruitment of preosteoclasts

Chemokines are chemotactic and modulate cellular functions in bone remodeling. Moreover, abundant levels of CXCR5, but very low levels of CXCL13 expression in differentiating osteoclasts have been reported 27. We therefore, examined a potential chemotactic role for CXCL13 expression in OSCC tumor cells in chemotaxis for human peripheral blood-derived osteoclast progenitor cells using a transwell system as described in methods. Recombinant CXCL13 protein dose-dependently stimulated chemotaxis of peripheral blood monocytes in 1 h at 10 ng/ml concentration (126±15 *versus* 37±6 in control) (Fig. 4A). This migration was significantly inhibited in the presence of anti-CXCR5 receptor antibody (Fig. 4B). These

results indicate that the CXCL13/CXCR5 axis may be critical in chemo-attraction of preosteoclast cells which facilitates osteoclast differentiation.

OSCC tumor invasion/osteolysis in vivo

To further examine the molecular mechanisms associated with OSCC tumor cell invasion and osteolysis of bone, we established an *in vivo* model for OSCC by subcutaneous injection of OSCC cells (SCC14a, SCC1 and SCC12) onto the surface of calvaria (7×10^6 cells in PBS) in NCr-nu/nu athymic mice. Tumors appeared by day seven and thereafter continued to grow for 4–5 weeks. The tumor size was measured at regular intervals with vernier calipers. All the OSCC cell lines demonstrated tumor development, however SCC14a cells with high tumor growth compared to SCC1 and SCC12 cell lines (Fig. 5A) and athymic mice with vehicle (PBS) control and SCC14a tumor-bearing mice are shown in Fig. 5B. After tumors reached 2000 mm^3 the mice were sacrificed and the isolated calvaria were subjected to μCT and histological analysis. μCT imaging analysis revealed numerous osteolytic lesions in calvaria isolated from OSCC tumor bearing mice. The increased rate of osteolysis in SCC14a tumor bearing mice compared to SCC12 could be related to high level production of CXCL13 (118 pg/ml) in these cells (Fig. 5C).

Histologic analysis of calvaria derived from tumor-bearing mice revealed tumor cell invasion into the bone matrix. Histochemical staining for TRAP activity identified a significant increase in the numbers of TRAP-positive osteoclasts at the tumor-bone interface compared to control mice. (Fig. 6A–D). The sections were analyzed by immunohistochemical staining to further confirm the expression of CXCL13/CXCR5 in tumor cells *in vivo*. As shown in Fig. 6E, tumor cells showed positive immunocytochemical staining with antibodies against CXCL13 and CXCR5. Tumor cells also stained positive for MMP-9 expression. In contrast, a control IgG did not stain. To further determine the potential of CXCL13 in OSCC tumor osteolysis, we developed SCC14a cells stably transfected with vectors containing control scrambled shRNA and shRNA against CXCL13 by lipofectamine and clonal cell lines were established by selection with neomycin (800 μg/ml). shRNA suppression of CXCL13 production and mRNA expression were confirmed by ELISA and real-time RT-PCR respectively (Fig. 5E&D). As shown in Fig. 5F, calvaria from SCC14a cells knock-down of CXCL13 expression demonstrated a significant decrease (52%) in tumor osteolysis compared to control scrambled shRNA transfected cells, however no change in tumor size. Further, histologic analysis of calvaria from SCC14a cells shRNA knock-down for CXCL13 tumor bearing mice showed inhibition of tumor invasion into bone matrix and significant decrease in osteoclasts number at tumor-bone interface compared to control scrambled shRNA transfected cells (Fig. 6F&G). Taken together, our results implicate CXCL13 play an important role in OSCC tumor invasion and osteolysis *in vivo*.

Discussion

Chemokines have a profound influence on bone remodeling in pathologic conditions. Recent studies indicated that down regulation of CXCL5 inhibits SCC carcinogenesis and that CXCL8 modulates cellular proliferation and migration involved in HNSCC tumor progression 28. Studies also implicated chemokine CXCL12 (SDF-1) and its receptor CXCR4 in migration and homing of multiple myeloma cells to the bone environment 20. SDF-1/CXCR4 signaling has been shown to be involved in lymph node metastasis in OSCC 29. Therefore, it is necessary to define a pathologic role for tumor-derived factors in bone invasion and the osteolysis process. In this study, we identified CXCL13/CXCR5 receptor expression and an autocrine regulation of CXCR5 receptor expression in OSCC cells. Furthermore, autocrine/paracrine activation of chemokine receptor-7 (CCR7) in HNSCC has been shown to mediate cell survival and metastasis 30. Inflammatory cytokines such as

IL-1β have been shown to induce CXCL13 production in differentiated osteoblasts 31 and human osteoblasts have been shown to express functional CXCR3 and 5 receptors 32. Also, CXCL12 (SDF-1) and CXCL13 (BCA-1) chemokines have been shown to directly modulate proliferation and type I collagen expression in osteoblastic cells in osteoarthritis 33. Therefore, high levels of CXCL13 production by OSCC cells could modulate osteoclast activity and gene expression in the tumor-bone environment. NF-κB has been shown to be constitutively activated in SCC and inactivation of NF-κB has been shown to suppress a malignant phenotype 34. In the present study, we show OSCC production of soluble RANKL and that CXCL13 chemotaxis of preosteoclast cells stimulated osteoclast differentiation. Similarly, SDF-1 binding to the CXCR4 receptor on human osteoclast precursor cells has been shown to` promote chemotactic recruitment, development and survival of osteoclasts 20. However, co-cultures of human OSCC cells (BHY and HSC-2 cells) with primary osteoblasts indicated suppression of OPG expression which is implicated in osteoclast differentiation35. Thus, it is possible that OSCC cells may inhibit OPG expression in the tumor-bone environment to enhance osteoclastogenesis and osteolytic activity. Conversely, bone derived SDF-1 from osteoblastic cells has been shown to stimulate IL-6 release from oral cancer cells which promotes osteoclastogenesis 36.

Previously it has been reported that IL-8 in saliva and IL-6 in serum are potential biomarkers for oral cancers 37. MMPs have been implicated in tumor invasion and metastasis of carcinomas. IL-8 secreted by OSCC has been shown to contribute to tumor cell invasion through modulation of MMP-7 expression in tumor cells 38. Furthermore, MMP-7 produced by osteoclasts at the prostate tumor-bone interface in a rodent model has been shown to promote osteolysis through solubilization of RANKL 39. Therefore, our findings that OSCC produces soluble RANKL which stimulated osteoclast differentiation and that CXCL13 induces high levels of MMP-9 expression in tumor cells suggests that CXCL13 plays an important role in OSCC bone invasion/osteolysis. We found no significant change in the levels of MMP-9 mRNA expression in CXCL13 treated cells in the presence of actinomycin D (data not shown), which suggests transcriptional regulation of MMP-9 expression. However, we cannot exclude the possibility that other factors produced by OSCC cells such as PTHrP and TNF-α may potentiate the actions of CXCL13 to stimulate osteoclast formation. Cytokines such as TNF-α and TGF-β1 have been shown to promote oral cancer invasion through upregulation of MMP-9 expression 40. The *in vivo* model that we developed of OSCC over calvaria in athymic mice mimicked tumor invasion and osteolysis by activated osteoclasts and abundant expression of CXCL13 and MMP-9 by tumor cells in the bone environment. Furthermore, increased rate of osteolysis observed with SCC14a cells which produce high levels of CXCL13 compared to SCC12 could implicate CXCL13 as a prognostic marker of OSCC tumor growth/osteolysis. Also, our findings that shRNA knock-down of CXCL13 expression in OSCC cells results in a significant decrease in tumor osteolysis further suggests CXCL13 as a therapeutic target for OSCC tumor osteolysis *in vivo*. The calvaria model of OSCC offers advantages for further unraveling the molecular mechanisms associated with osteoclast activation at the tumor-bone interface in a stage-specific manner. Thus, our results implicate a functional role for CXCL13 in OSCC tumor invasion into bone and may be a potential therapeutic target for prevention of osteolysis associated with OSCC *in vivo*.

Acknowledgments

Grant support: This work was conducted in a facility constructed with support from the National Institutes of Health, Grant Number C06 RR015455 from the Extramural Research Facilities Program of the National Center for Research Resources.

We thank Saeed ElOjeimy for his assistance with the athymic mice.

References

1. Funk GF, Karnell LH, Robinson RA, Zhen WK, Trask DK, Hoffman HT. Presentation, treatment, and outcome of oral cavity cancer: a National Cancer Data Base report. Head Neck. 2002; 24:165–80. [PubMed: 11891947]
2. Choi S, Myers JN. Molecular pathogenesis of oral squamous cell carcinoma: implications for therapy. J Dent Res. 2008; 87:14–32. [PubMed: 18096889]
3. LoTempio MM, Veena MS, Steele HL, Ramamurthy B, Ramalingam TS, Cohen AN, Chakrabarti R, Srivatsan ES, Wang MB. Curcumin suppresses growth of head and neck squamous cell carcinoma. Clin Cancer Res. 2005; 11:6994–7002. [PubMed: 16203793]
4. ElOjeimy S, McKillop JC, El-Zawahry AM, Holman DH, Liu X, Schwartz DA, Day TA, Dong JY, Norris JS. FasL gene therapy: a new therapeutic modality for head and neck cancer. Cancer Gene Ther. 2006; 13:739–45. [PubMed: 16543918]
5. Nelson K, Helmstaedter V, Lage H. The influence of tamoxifen on growth behavior and cell-cell adhesion in OSCC in vitro. Oral Oncol. 2007; 43:720–7. [PubMed: 17112777]
6. Senkal CE, Ponnusamy S, Rossi MJ, Bialewski J, Sinha D, Jiang JC, Jazwinski SM, Hannun YA, Ogretmen B. Role of human longevity assurance gene 1 and C18-ceramide in chemotherapy-induced cell death in human head and neck squamous cell carcinomas. Mol Cancer Ther. 2007; 6:712–22. [PubMed: 17308067]
7. Hsu H, Lacey DL, Dunstan CR, Solovyev I, Colombero A, Timms E, Tan HL, Elliott G, Kelley MJ, Sarosi I, Wang L, Xia XZ, et al. Tumor necrosis factor receptor family member RANK mediates osteoclast differentiation and activation induced by osteoprotegerin ligand. Proc Natl Acad Sci U S A. 1999; 96:3540–5. [PubMed: 10097072]
8. Reddy SV. Regulatory mechanisms operative in osteoclasts. Crit Rev Eukaryot Gene Expr. 2004; 14:255–70. [PubMed: 15663356]
9. Nomura T, Shibahara T, Katakura A, Matsubara S, Takano N. Establishment of a murine model of bone invasion by oral squamous cell carcinoma. Oral Oncol. 2007; 43:257–62. [PubMed: 16920384]
10. Deyama Y, Tei K, Yoshimura Y, Izumiyama Y, Takeyama S, Hatta M, Totsuka Y, Suzuki K. Oral squamous cell carcinomas stimulate osteoclast differentiation. Oncol Rep. 2008; 20:663–8. [PubMed: 18695921]
11. Zlotnik A, Yoshie O. Chemokines: a new classification system and their role in immunity. Immunity. 2000; 12:121–7. [PubMed: 10714678]
12. Belperio JA, Keane MP, Arenberg DA, Addison CL, Ehlert JE, Burdick MD, Strieter RM. CXC chemokines in angiogenesis. J Leukoc Biol. 2000; 68:1–8. [PubMed: 10914483]
13. Muller A, Homey B, Soto H, Ge N, Catron D, Buchanan ME, McClanahan T, Murphy E, Yuan W, Wagner SN, Barrera JL, Mohar A, et al. Involvement of chemokine receptors in breast cancer metastasis. Nature. 2001; 410:50–6. [PubMed: 11242036]
14. Muller A, Sonkoly E, Eulert C, Gerber PA, Kubitza R, Schirlau K, Franken-Kunkel P, Poremba C, Snyderman C, Klotz LO, Ruzicka T, Bier H, et al. Chemokine receptors in head and neck cancer: association with metastatic spread and regulation during chemotherapy. Int J Cancer. 2006; 118:2147–57. [PubMed: 16331601]
15. Legler DF, Loetscher M, Roos RS, Clark-Lewis I, Baggiolini M, Moser B. B cell-attracting chemokine 1, a human CXC chemokine expressed in lymphoid tissues, selectively attracts B lymphocytes via BLR1/CXCR5. J Exp Med. 1998; 187:655–60. [PubMed: 9463416]
16. Ziober AF, Patel KR, Alawi F, Gimotty P, Weber RS, Feldman MM, Chalian AA, Weinstein GS, Hunt J, Ziober BL. Identification of a gene signature for rapid screening of oral squamous cell carcinoma. Clin Cancer Res. 2006; 12:5960–71. [PubMed: 17062667]
17. Srinivasan S, Ito M, Kajiya H, Key LL Jr, Johnson-Pais TL, Reddy SV. Functional characterization of human osteoclast inhibitory peptide-1 (OIP-1/hSca) gene promoter. Gene. 2006; 371:16–24. [PubMed: 16380218]
18. Susa M, Luong-Nguyen NH, Cappellen D, Zamurovic N, Gamse R. Human primary osteoclasts: in vitro generation and applications as pharmacological and clinical assay. J Transl Med. 2004; 2:6. [PubMed: 15025786]

19. Shanmugarajan S, Irie K, Musselwhite C, Key LL Jr, Ries WL, Reddy SV. Transgenic mice with OIP-1/hSca overexpression targeted to the osteoclast lineage develop an osteopetrosis bone phenotype. J Pathol. 2007; 213:420–8. [PubMed: 17940999]
20. Wright LM, Maloney W, Yu X, Kindle L, Collin-Osdoby P, Osdoby P. Stromal cell-derived factor-1 binding to its chemokine receptor CXCR4 on precursor cells promotes the chemotactic recruitment, development and survival of human osteoclasts. Bone. 2005; 36:840–53. [PubMed: 15794931]
21. Sundaram K, Nishimura R, Senn J, Youssef RF, London SD, Reddy SV. RANK ligand signaling modulates the matrix metalloproteinase-9 gene expression during osteoclast differentiation. Exp Cell Res. 2007; 313:168–78. [PubMed: 17084841]
22. Krieg C, Boyman O. The role of chemokines in cancer immune surveillance by the adaptive immune system. Seminars in cancer biology. 2008
23. Miyazaki H, Patel V, Wang H, Edmunds RK, Gutkind JS, Yeudall WA. Down-regulation of CXCL5 inhibits squamous carcinogenesis. Cancer Res. 2006; 66:4279–84. [PubMed: 16618752]
24. Tada T, Shin M, Fukushima H, Okabe K, Ozeki S, Okamoto M, Jimi E. Oral squamous cell carcinoma cells modulate osteoclast function by RANKL-dependent and -independent mechanisms. Cancer letters. 2008
25. Blair JM, Zhou H, Seibel MJ, Dunstan CR. Mechanisms of disease: roles of OPG, RANKL and RANK in the pathophysiology of skeletal metastasis. Nature clinical practice. 2006; 3:41–9.
26. Sun L, Diamond ME, Ottaviano AJ, Joseph MJ, Ananthanarayan V, Munshi HG. Transforming growth factor-beta 1 promotes matrix metalloproteinase-9-mediated oral cancer invasion through snail expression. Mol Cancer Res. 2008; 6:10–20. [PubMed: 18234959]
27. Grassi F, Piacentini A, Cristino S, Toneguzzi S, Cavallo C, Facchini A, Lisignoli G. Human osteoclasts express different CXC chemokines depending on cell culture substrate: molecular and immunocytochemical evidence of high levels of CXCL10 and CXCL12. Histochem Cell Biol. 2003; 120:391–400. [PubMed: 14600836]
28. Christofakis EP, Miyazaki H, Rubink DS, Yeudall WA. Roles of CXCL8 in squamous cell carcinoma proliferation and migration. Oral Oncol. 2008; 44:920–6. [PubMed: 18282785]
29. Uchida D, Begum NM, Almofti A, Nakashiro K, Kawamata H, Tateishi Y, Hamakawa H, Yoshida H, Sato M. Possible role of stromal-cell-derived factor-1/CXCR4 signaling on lymph node metastasis of oral squamous cell carcinoma. Exp Cell Res. 2003; 290:289–302. [PubMed: 14567988]
30. Wang J, Seethala RR, Zhang Q, Gooding W, van Waes C, Hasegawa H, Ferris RL. Autocrine and paracrine chemokine receptor 7 activation in head and neck cancer: implications for therapy. J Natl Cancer Inst. 2008; 100:502–12. [PubMed: 18364504]
31. Lisignoli G, Cristino S, Toneguzzi S, Grassi F, Piacentini A, Cavallo C, Facchini A, Mariani E. IL1beta and TNFalpha differently modulate CXCL13 chemokine in stromal cells and osteoblasts isolated from osteoarthritis patients: evidence of changes associated to cell maturation. Exp Gerontol. 2004; 39:659–65. [PubMed: 15050303]
32. Lisignoli G, Toneguzzi S, Piacentini A, Cattini L, Lenti A, Tschon M, Cristino S, Grassi F, Facchini A. Human osteoblasts express functional CXC chemokine receptors 3 and 5: activation by their ligands, CXCL10 and CXCL13, significantly induces alkaline phosphatase and beta-N-acetylhexosaminidase release. J Cell Physiol. 2003; 194:71–9. [PubMed: 12447991]
33. Lisignoli G, Toneguzzi S, Piacentini A, Cristino S, Grassi F, Cavallo C, Facchini A. CXCL12 (SDF-1) and CXCL13 (BCA-1) chemokines significantly induce proliferation and collagen type I expression in osteoblasts from osteoarthritis patients. J Cell Physiol. 2006; 206:78–85. [PubMed: 15965952]
34. Loercher A, Lee TL, Ricker JL, Howard A, Geoghegen J, Chen Z, Sunwoo JB, Sitcheran R, Chuang EY, Mitchell JB, Baldwin AS Jr, Van Waes C. Nuclear factor-kappaB is an important modulator of the altered gene expression profile and malignant phenotype in squamous cell carcinoma. Cancer Res. 2004; 64:6511–23. [PubMed: 15374962]
35. Tada T, Jimi E, Okamoto M, Ozeki S, Okabe K. Oral squamous cell carcinoma cells induce osteoclast differentiation by suppression of osteoprotegerin expression in osteoblasts. Int J Cancer. 2005; 116:253–62. [PubMed: 15800904]

36. Tang CH, Chuang JY, Fong YC, Maa MC, Way TD, Hung CH. Bone-derived SDF-1 stimulates IL-6 release via CXCR4, ERK and NF-kappaB pathways and promotes osteoclastogenesis in human oral cancer cells. Carcinogenesis. 2008; 29:1483–92. [PubMed: 18310089]

37. St John MA, Li Y, Zhou X, Denny P, Ho CM, Montemagno C, Shi W, Qi F, Wu B, Sinha U, Jordan R, Wolinsky L, et al. Interleukin 6 and interleukin 8 as potential biomarkers for oral cavity and oropharyngeal squamous cell carcinoma. Arch Otolaryngol Head Neck Surg. 2004; 130:929–35. [PubMed: 15313862]

38. Watanabe H, Iwase M, Ohashi M, Nagumo M. Role of interleukin-8 secreted from human oral squamous cell carcinoma cell lines. Oral Oncol. 2002; 38:670–9. [PubMed: 12167419]

39. Lynch CC, Hikosaka A, Acuff HB, Martin MD, Kawai N, Singh RK, Vargo-Gogola TC, Begtrup JL, Peterson TE, Fingleton B, Shirai T, Matrisian LM, et al. MMP-7 promotes prostate cancer-induced osteolysis via the solubilization of RANKL. Cancer Cell. 2005; 7:485–96. [PubMed: 15894268]

40. Hohberger L, Wuertz BR, Xie H, Griffin T, Ondrey F. TNF-alpha drives matrix metalloproteinase-9 in squamous oral carcinogenesis. Laryngoscope. 2008; 118:1395–9. [PubMed: 18496150]

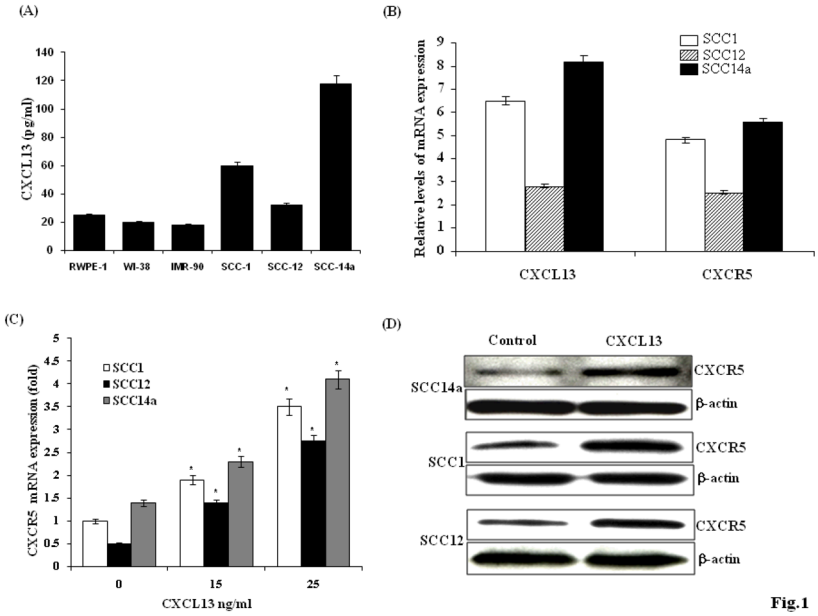

Figure 1.

CXCL13/CXCR5 expression in human OSCC cells. (A). CXCL13 levels in conditioned media (CM) obtained from OSCC cells (SCC14a, SCC12, SCC1), normal epithelial cells (RWPE-1) and normal fibroblast cells (WI-38 and IMR-90) as measured by ELISA. (B). Real-time RT-PCR analysis of CXCL13 and CXCR5 receptor expression relative to the level of GAPDH amplification in OSCC cells. (C) CXCL13 stimulates CXCR5 mRNA expression in OSCC cells. The cells were stimulated with different concentrations of CXCL13 (0–25 ng/ml) for 48 h. Total RNA was isolated from these cells and CXCR5 mRNA expression was quantified by Real time RT-PCR analysis (*$p<0.05$). (D) Western blot analysis of CXCR5 expression in CXCL13 stimulated OSCC cells.

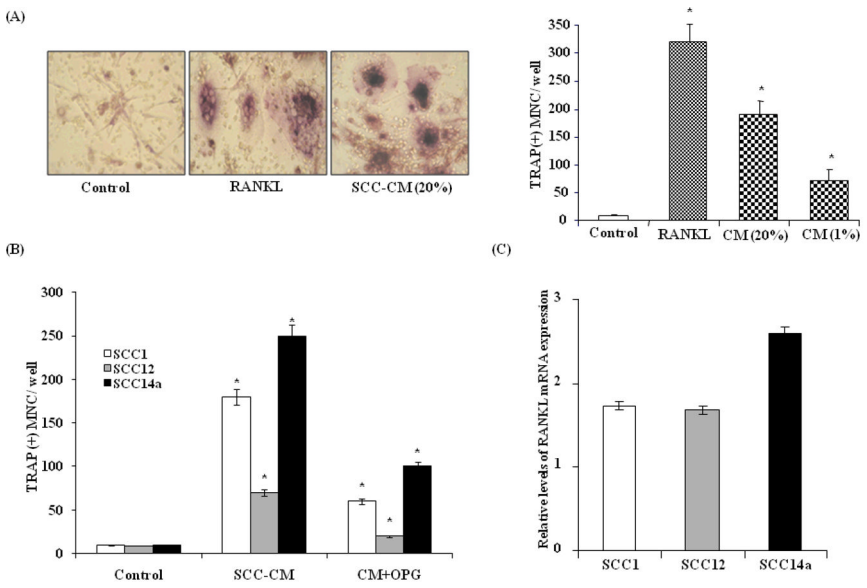

Figure 2.

Conditioned media (CM) from OSCC cells stimulates osteoclastogenesis. (A) SCC14a cell CM induced osteoclast differentiation in human peripheral blood monocyte (PBMC) culture. PBMC were incubated with RANKL (100 ng/ml) or SCC-CM (1 and 20%) in the presence of M-CSF (10 ng/ml) for 10 days. Cells cultured with M-CSF alone served as control. TRAP-positive multinucleated osteoclasts formed at the end of the culture period were scored (*$p<0.05$). (B) Osteoprotegerin (OPG) inhibition of OSCC-CM stimulated osteoclast differentiation in PBMC cultures. PBMC cultured with OSCC-CM (20%) with and without OPG (100 ng/ml) for 10 days. PBMC cultured with M-CSF alone served as control. TRAP positive multinucleated cells formed at the end of the culture period were scored (*$p<0.05$). (C) Real-time RT-PCR analysis of RANKL mRNA expression in OSCC cells. Relative mRNA expression level was normalized with respect to GAPDH amplification (*$p<0.05$).

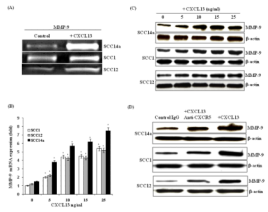

Figure 3.

CXCL13 stimulates MMP-9 expression in OSCC cells. (A) Gelatin zymogram analysis of MMP-9 activity in CM obtained from OSCC cells (SCC14a, SCC1 and SCC12) were stimulated with and without CXCL13 (10 ng/ml) for 48 h. (B) OSCC cells were stimulated with and without CXCL13 (0–25 ng/ml) for 48 h. Total RNA isolated from these cells was analyzed for MMP-9 mRNA expression by real-time RT-PCR. Relative levels of MMP-9 mRNA expression was normalized with respect to the level of GAPDH amplification (*$p<0.05$). (C) OSCC cells were stimulated with CXCL13 (0–25 ng/ml) for 48 h and total cell lysates were analyzed by Western blot for MMP-9 expression. (D) Anti-CXCR5 antibody inhibits CXCL13-induced MMP-9 expression in OSCC cells. Rabbit non-specific IgG treatment severed as control.

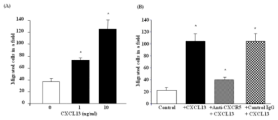

Figure 4.

Recombinant hCXCL13 protein induced chemotaxis of peripheral blood monocyte cells (PBMC). (A). PBMC were treated with CXCL13 (0–10 ng/ml) and chemotaxis was assayed as described in the methods. (B). PBMC were incubated with anti-CXCR5 antibody (25 ng/ml) for 1 h and stimulated with CXCL13 (10 ng/ml) (*$p<0.05$). Cells cultured in the absence of CXCL13 or CXCL13 treatment in the presence of rabbit non-specific IgG served as controls.

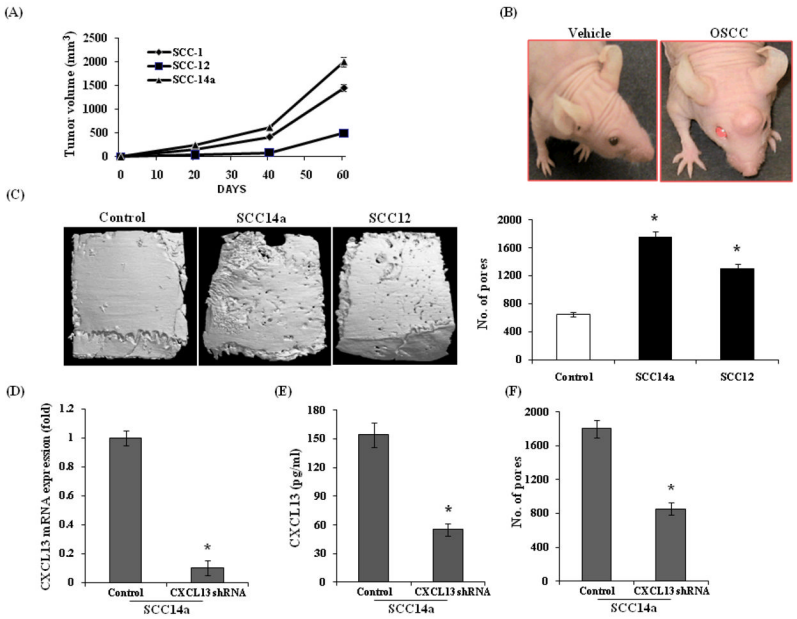

Figure 5.

In vivo model of OSCC tumor invasion/osteolysis in athymic mice. (A) Athymic mice were subcutaneously injected with 7×10^6 OSCC cells (SCC1, SCC12 and SCC14a) in PBS over calvaria. Tumors were allowed to grow for 4–5 weeks and tumor volumes were measured using vernier calipers (*$p<0.05$). (B) Athymic mice with vehicle (PBS) control and SCC14a tumor. (C) μCT analysis of calvaria isolated from OSCC tumor-bearing athymic mice. Mice were injected with 7×10^6 SCC14a, SCC12 and PBS (control) over calvaria was sacrificed after 4–5 weeks and calvaria isolated from these mice were μCT analyzed for osteolytic lesions. (D) Real-time RT-PCR analysis of CXCL13 mRNA expression in control scrambled shRNA and CXCL13 shRNA (SABiosciences, Frederick, MD) knock-down SCC14a cells. Relative mRNA expression level was normalized with respect to GAPDH amplification (*$p<0.05$). (E) CXCL13 levels in conditioned media (CM) obtained from control and CXCL13 shRNA knock-down SCC14a cells as measured by ELISA (*$p<0.05$). (F)μCT analysis of osteolytic lesions in calvaria isolated from control and CXCL13 shRNA knock-down SCC14a tumor-bearing athymic mice (*$p<0.05$).

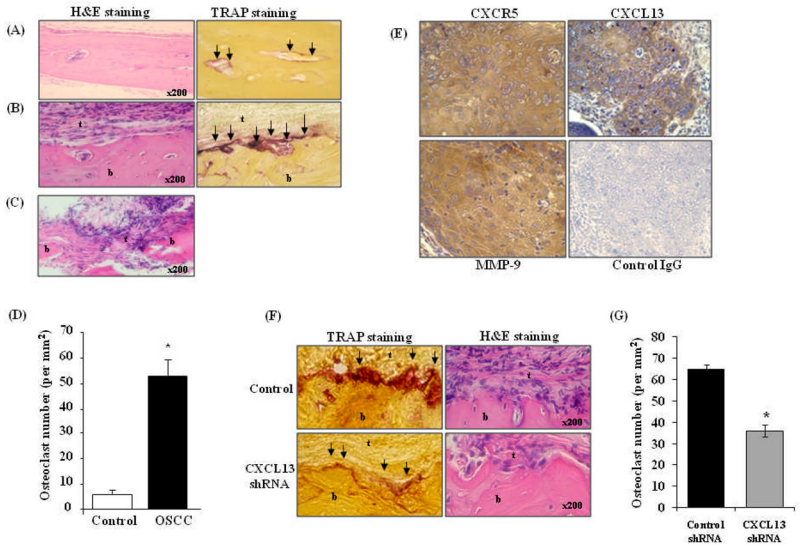

Figure 6.

Histological analysis of calvaria excised from control and OSCC tumor bearing mice. Histochemical staining was performed with hematoxylin-eosin (H&E) and for TRAP activity. (A). Calvaria from control mice. (B). OSCC tumor bearing mouse calvaria. (C) OSCC tumor invasion into calvarial bone (arrows point to TRAP- positive osteoclasts; b= bone, t= tumor). (D) Osteoclasts at the tumor-bone interface and in calvaria from control mice treated with PBS alone were counted using a micrometer scale and expressed per mm^2 (*$p<0.05$) (E) Immuno histochemical analysis of CXCR5, CXCL13 and MMP-9 expression in SCC14a tumors from athymic mice. Immunostaining with antibodies specific to CXCR5, CXCL13 and MMP-9 was performed and a rabbit non-specific IgG served as control. (F) Histochemical staining of calvaria isolated from control scrambled shRNA, CXCL13 shRNA knock-down SCC14a cell tumor-bearing athymic mice were performed with H&E and TRAP activity staining for osteoclasts (G) Osteoclasts numbers in the control and CXCL13 shRNA knock-down tumor-bone interface were counted using a micrometer scale and expressed per mm^2 (*$p<0.05$).